

Devil's vortex-lenses

Walter D. Furlan^{1*}, Fernando Giménez², Arnau Calatayud³ and Juan A. Monsoriu³

¹Departamento de Óptica, Universitat de València, E-46100 Burjassot, Spain

²Instituto de Matemática Pura y Aplicada, Universidad Politécnica de Valencia, E-46022 Valencia, Spain

³Centro de Tecnologías Físicas, Universidad Politécnica de Valencia, E-46022 Valencia, Spain

*walter.furlan@uv.es

Abstract: In this paper we present a new kind of vortex lenses in which the radial phase distribution is characterized by the “devil’s staircase” function. The focusing properties of these fractal DOEs coined *Devil’s vortex-lenses* are analytically studied and the influence of the topological charge is investigated. It is shown that under monochromatic illumination a vortex devil’s lens give rise a focal volume containing a delimited chain of vortices that are axially distributed according to the self-similarity of the lens.

©2009 Optical Society of America

OCIS codes: (050.1940) diffraction; (050.1970) diffractive optics;

References and Links

1. F. S. Roux, “Distribution of angular momentum and vortex morphology in optical beams,” *Opt. Commun.* **242**(1–3), 45–55 (2004).
2. G. Gbur, and T. D. Visser, “Phase singularities and coherence vortices in linear optical systems,” *Opt. Commun.* **259**(2), 428–435 (2006).
3. N. R. Heckenberg, R. McDuff, C. P. Smith, and A. G. White, “Generation of optical phase singularities by computer-generated holograms,” *Opt. Lett.* **17**(3), 221–223 (1992).
4. W. M. Lee, X. C. Yuan, and W. C. Cheong, “Optical vortex beam shaping by use of highly efficient irregular spiral phase plates for optical micromanipulation,” *Opt. Lett.* **29**(15), 1796–1798 (2004).
5. S. H. Tao, X.-C. Yuan, J. Lin, and R. Burge, “Sequence of focused optical vortices generated by a spiral fractal zone plates,” *Appl. Phys. Lett.* **89**(3), 031105 (2006).
6. G. Saavedra, W. D. Furlan, and J. A. Monsoriu, “Fractal zone plates,” *Opt. Lett.* **28**(12), 971–973 (2003).
7. J. A. Monsoriu, G. Saavedra, and W. D. Furlan, “Fractal zone plates with variable lacunarity,” *Opt. Express* **12**(18), 4227–4234 (2004), <http://www.opticsinfobase.org/abstract.cfm?URI=oe-12-18-4227>.
8. J. A. Davis, L. Ramirez, J. A. Martín-Romo, T. Alieva, and M. L. Calvo, “Focusing properties of fractal zone plates: experimental implementation with a liquid-crystal display,” *Opt. Lett.* **29**(12), 1321–1323 (2004).
9. H.-T. Dai, X. Wang, and K.-S. Xu, “Focusing properties of fractal zone plates with variable lacunarity: experimental studies based on liquid crystal on silicon,” *Chin. Phys. Lett.* **22**(11), 2851–2854 (2005).
10. C. Martelli, and J. Canning, “Fresnel Fibres with Omnidirectional Zone Cross-sections,” *Opt. Express* **15**(7), 4281–4286 (2007), <http://www.opticsinfobase.org/oe/abstract.cfm?URI=oe-15-7-4281>.
11. F. Giménez, J. A. Monsoriu, W. D. Furlan, and A. Pons, “Fractal photon sieve,” *Opt. Express* **14**(25), 11958–11963 (2006), <http://www.opticsinfobase.org/oe/abstract.cfm?URI=oe-14-25-11958>.
12. J. A. Monsoriu, W. D. Furlan, G. Saavedra, and F. Giménez, “Devil’s lenses,” *Opt. Express* **15**(21), 13858–13864 (2007), <http://www.opticsinfobase.org/oe/abstract.cfm?URI=oe-15-21-13858>.
13. D. R. Chalice, “A characterization of the Cantor function,” *Am. Math. Mon.* **98**(3), 255–258 (1991).
14. F. Doveil, A. Macor, and Y. Elskens, “Direct observation of a devil’s staircase in wave-particle interaction,” *Chaos* **16**(3), 033103 (2006).
15. M. Hupalo, J. Schmalian, and M. C. Tringides, “Devil’s staircase” in Pb/Si(111) ordered phases,” *Phys. Rev. Lett.* **90**(21), 216106 (2003).
16. Y. F. Chen, T. H. Lu, K. W. Su, and K. F. Huang, “Devil’s staircase in three-dimensional coherent waves localized on Lissajous parametric surfaces,” *Phys. Rev. Lett.* **96**(21), 213902 (2006).
17. D. Wu, L.-G. Niu, Q.-D. Chen, R. Wang, and H.-B. Sun, “High efficiency multilevel phase-type fractal zone plates,” *Opt. Lett.* **33**(24), 2913–2915 (2008).
18. G. A. Swartzlander, Jr., “Peering into darkness with a vortex spatial filter,” *Opt. Lett.* **26**(8), 497–499 (2001).
19. K. Crabtree, J. A. Davis, and I. Moreno, “Optical processing with vortex-producing lenses,” *Appl. Opt.* **43**(6), 1360–1367 (2004).

1. Introduction

Optical vortices extended the capabilities of conventional optical traps because in addition to trap microparticles they are capable to set these particles into rotation due to the orbital angular momentum of light [1,2]. Among the several methods that have been proposed for optical vortices generation the most common approach is the spiral phase plate [3,4] mainly

inasmuch as this technique provides a high energy efficiency. Recently, a method for producing a sequence of focused optical vortices along the propagation direction has been proposed by the use of a *spiral fractal zone plate* [5]. Fractal zone plates (FraZPs) are binary zone plates with fractal profile along the square of the radial coordinate [6,7]. These new optical elements have deserved the attention of several experimental research groups working in diffractive optics [8,9] and, besides of the above mentioned spiral fractal zone plates, they also inspired the invention of other photonic structures such as optical fibers with fractal cross section [10] and fractal photon sieves [11].

It has been demonstrated that for multiple-plane optical trappings, the spiral FraZP provides the potential to generate a light beam with hybrid axial optical vortices and multiple subsidiary foci near the major focal points [5], and this method was proposed for optical trapping with focused vortices in the microscopic scale with high focal depth. Since the diffraction efficiency of diffractive optical elements (DOEs) is crucial for certain practical applications and to further improve it for a spiral FraZP, in this paper, we propose a new design of spiral phase plate which is based on a blazed FraZP: the Devil's lens (DLs) [12]. A DL lens has a characteristic surface relief which is obtained using the *devil's staircase* function [13]. This function, which is related to the standard Cantor set, also appears in several areas of physics, as for instance, in wave-particle interactions [14], in crystal growth [15], and in the mode locking of the 3D coherent states in high-Q laser cavities [16]. A multilevel phase version of a DL has been reported experimentally recently [17].

The new element we propose, which is referred to as *Devil's vortex-lens* (DVL), is a phase-only Devil's lens modulated by an helical phase structure. Our design is able to generate a sequence of focused vortices surrounding the major foci inside a single main fractal focus. It is because of its blazed profile that DVL has an improved diffraction efficiency with respect to the spiral fractal zone. The focusing properties of different DVLs are studied by computing the intensity distribution along the optical axis and the transverse diffraction patterns along the propagation direction.

2. Vortex devil's lenses design

The design of a Devil's lens is mathematically based on the Cantor function [12,13], which is defined in the domain [0,1] as

$$F_s(x) = \begin{cases} \frac{1}{2^s} & \text{if } p_{s,l} \leq x \leq q_{s,l} \\ \frac{1}{2^s} \frac{x - q_{s,l}}{p_{s,l+1} - q_{s,l}} + \frac{l}{2^s} & \text{if } q_{s,l} \leq x \leq p_{s,l+1} \end{cases}, \quad (1)$$

being $F_s(0) = 0$ and $F_s(1) = 1$. In Fig. 1 we have represented the triadic Cantor function $F_3(x)$. It can be seen that the steps of the devil's staircase, take the constant values $l/2^3$ in the intervals $p_{3,l} \leq x \leq q_{3,l}$ (with $l = 1, \dots, 7$) whereas in between these intervals the function increases linearly.

From a particular Cantor function $F_s(x)$ a DL is defined as a circularly symmetric pure-phase DOE whose transmittance is defined by

$$q(\zeta) = \exp[i\Phi_{DL}] = \exp[-i 2^{s+1} \pi F_s(\zeta)], \quad (2)$$

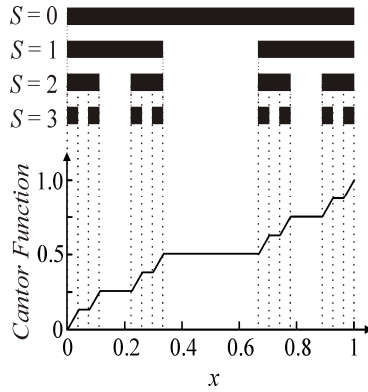


Fig. 1. Triadic Cantor set for $S = 1$, $S = 2$, and $S = 3$. The structure for $S = 0$ is the initiator and the one corresponding to $S = 1$ is the generator. The Cantor function or Devil's staircase, $F_S(x)$, is shown under the corresponding Cantor set for $S = 3$.

where

$$\zeta = (r/a)^2 \quad (3)$$

is the normalized quadratic radial variable and a is the lens radius. Thus, the phase variation along the radial coordinate is quadratic in each zone of the lens. At the gap regions defined by the Cantor set the phase shift is $-l2\pi$, with $l = 1, \dots, 2^S - 1$. The form of a DL is shown in Fig. 2a) in which the gray levels show the continuous phase variation.

A DVL can be simply constructed from a conventional DL by adding to it the azimuthal variation of the phase that characterize a vortex lens i.e.; $\Phi_{VL} = im\theta$, where m is a non zero integer called the topological charge and θ is the azimuthal angle. In this way the phase distribution of DVL is given by: $\Phi_{DVL} = \text{mod}_{2\pi}(\Phi_{DL} + \Phi_{VL})$ being Φ_{DL} the phase of the of a DL (see Eq. (2)). Figs. 2b) and 2c) show DVLs with $m = 1$ and $m = 3$, respectively. Note in the same figure that a Devil's lens is a DVL with $m = 0$. In other words: DVLs can be considered as a generalization of the DLs.

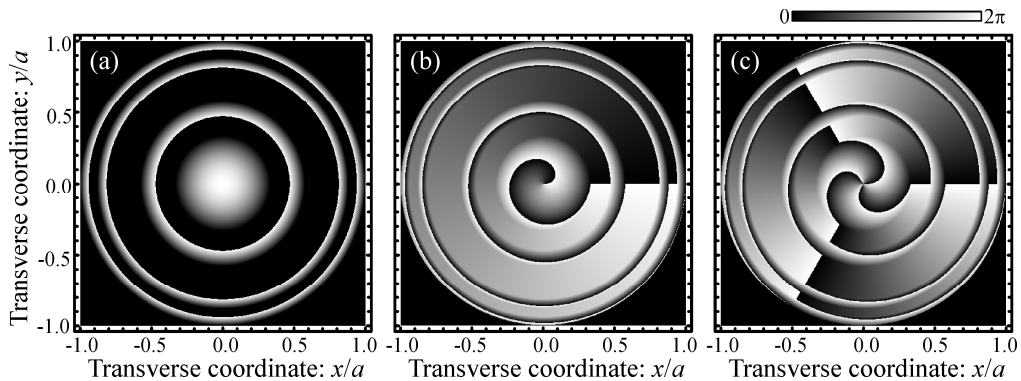


Fig. 2. (a) Phase variation as gray levels for a DL ($S = 2$), and for DVLs with topological charge (b) $m = 1$, and (c) $m = 3$.

3. Focusing properties of a DVL

Let us consider the diffraction pattern provided by a DVL. The transmittance of this lens, $t(r, \theta)$, can be expressed as the product of two factors, the first one, associated to a DL which has only a radial dependence and the other one corresponding to a vortex lens with a linear phase dependence on the azimuthal angle, i.e.;

$$t(r, \theta) = p(r) \exp[im\theta]. \quad (4)$$

Within the Fresnel approximation the diffracted field at a given point (z, r, θ) , where z is the axial distance from the pupil plane, can be characterized by the irradiance and the phase functions which are given respectively by:

$$I(z, r) = \left(\frac{2\pi}{\lambda z}\right)^2 \left| \int_0^a p(r_o) \exp\left(-i\frac{\pi}{\lambda z} r_o^2\right) J_m\left(\frac{2\pi r_o r}{\lambda z}\right) r_o dr_o \right|^2; \quad (5)$$

$$\Phi(z, r, \theta) = m\left(\theta + \frac{\pi}{2}\right) - \frac{2\pi}{\lambda} z - \frac{\pi r^2}{\lambda z} - \frac{\pi}{2}; \quad (6)$$

In Eqs. (5) and (6) λ is the wavelength of the incident monochromatic plane wave. Now, if the pupil transmittance is defined in terms of the normalized variable in Eq. (3), these equations become

$$I(u, v) = 4\pi^2 u^2 \left| \int_0^1 q(\zeta) \exp(-i2\pi u \zeta) J_m(4\pi \sqrt{\zeta uv}) d\zeta \right|^2, \quad (7)$$

$$\Phi(u, v, \theta) = m\left(\theta + \frac{\pi}{2}\right) - \frac{\pi a^2}{\lambda^2 u} - 2\pi uv^2 - \frac{\pi}{2}; \quad (8)$$

where $q(\zeta) = p(r_o)$ is given by Eq. (2), and $u = a^2/2\lambda z$ and $v = r/a$ are the reduced axial and transverse coordinates, respectively.

By using the above equations we have computed the irradiance provided by the DVLs shown in Fig. 2. The integrals were numerically evaluated using Simpson's rule using a step length 1/500. As expected, the axial response for the DL (Fig. 2a) represented in Fig. 3a) exhibits a single major focus at $f_s = a^2/2\lambda^3$ and a number of subsidiary focal points surrounding it, producing a focal volume with a characteristic fractal profile. Note that, if we change the topological charge, each focus transforms into a vortex and a chain of doughnut shaped foci is generated. Figs. 3(b) and 3(c) shows the focal volume associated to the DVL with $m = 1$ and $m = 3$, respectively. We have also computed the diffraction patterns for different topological charges (not shown) and verified that the diameter of the doughnut increases with the topological charge as happens with conventional vortex producing lenses [18, 19].

For predicting the focusing capabilities of the DVLs, the diffracted wavefield, over the whole transverse plane is of interest mainly because it can reflect the phase variations of the field from plane to plane. Eq. (5) has been used to calculate the evolution of the diffraction patterns for a DVL ($S = 2$, $m = 1$) around the main vortex, $u = 9$ (Fig. 4a) and around the first subsidiary vortex, $u = 9.8$ (Fig. 4b). In both cases the range of the sampling for the axial coordinate is limited to $\Delta u = -10^{-7}$. In the animated Fig. 4 each frame represent the form of the transverse field contours as the product of the irradiance times the phase of the wavefront within the range $|x/a| < 0.15$, $|y/a| < 0.15$. The phase variations are in the range $[0, 2\pi]$, while the intensities are normalized to the maximum value at each transverse plane. In this way, the relative intensity at the vortices can be directly compared. These animations show the annular form of the transverse intensity and also the phase rotation with the axial coordinate. Note that due to the form of this representation only the changes in the phase are relevant since the intensity didn't change with time. The concentric rings are caused by constructive interferences of the different rings of the DVL. These are affected by the vortex as the whole diffraction pattern.

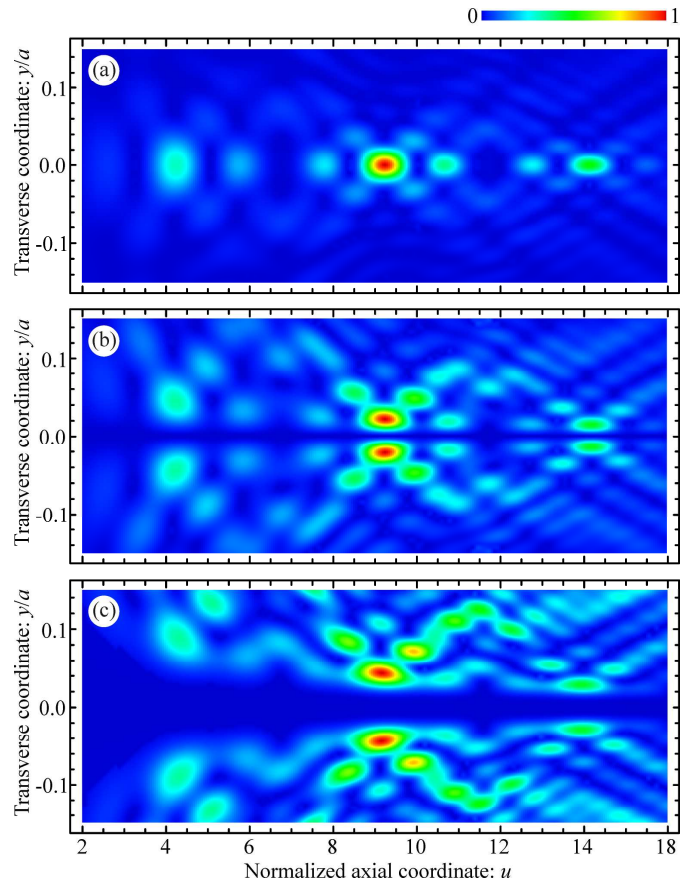


Fig. 3. Normalized irradiance contours computed for the lenses in Fig. 2. (a) $m = 0$, (b) $m = 1$, and (c) $m = 3$.

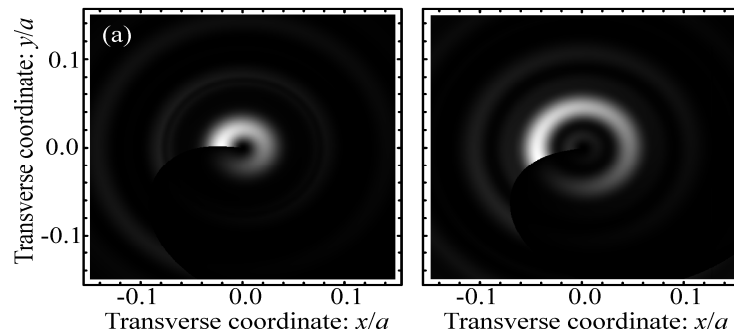


Fig. 4. Transverse field maps (as the product of the irradiance times phase) at (a) $u = 9$ and (b) $u = 9.8$ computed for the lens in Fig. 1(b) with $m = 1$. The animations Fig. 4a.avi ([Media 1](#), 1.62 MB) and Fig. 4b.avi ([Media 2](#), 2.18 MB) show the evolution of the vortices as they propagate along the optical axis.

4. Conclusions

A new type of vortex lenses, coined “devil’s vortex-lenses”, has been introduced. To avoid the losses that characterize the spiral fractal zone plates [5] and to improve their diffraction efficiency, the phase function for a typical devil’s vortex lens has a fractal blazed profile. It is well known that continuous phase profiles generally also have a better performance as

